UC Irvine
UC Irvine Previously Published Works

Title

Surface chlorophyll concentrations in relation to the Antarctic Polar Front: seasonal and spatial patterns from satellite observations

Permalink

https://escholarship.org/uc/item/5bp54127

Journal

Journal of Marine Systems, 37(1-3)

ISSN

0924-7963

Authors

Moore, J Keith
Abbott, Mark R

Publication Date

2002-11-01

DOI

10.1016/s0924-7963(02)00196-3

Peer reviewed

Surface chlorophyll concentrations in relation to the Antarctic Polar Front: seasonal and spatial patterns from satellite observations

J. Keith Moore[a,*], Mark R. Abbott[b]

[a] National Center for Atmospheric Research, NCAR, Climate and Global Dynamics, P.O. Box 3000, Boulder, CO 80307-3000, USA
[b] College of Oceanic and Atmospheric Sciences, Oregon State University, 104 Ocean Administration Building, Corvallis, OR 97331, USA

Abstract

Satellite ocean color data from the Sea Viewing Wide Field of View Sensor (SeaWiFS) are used to investigate phytoplankton bloom dynamics at the Antarctic Polar Front (PF). Satellite sea surface temperature (SST) data are used to map the location of the PF at weekly timescales. Elevated chlorophyll within the PF often appears as a narrow band that occupies only a portion of the SST gradient across the PF. Phytoplankton blooms within the PF occur most frequently during the month of December and are unevenly distributed within the Southern Ocean. Elevated chlorophyll concentrations at the PF are most frequently observed where the current is interacting with large topographic features.

Mesoscale physical processes, including meander-induced upwelling and increased eddy mixing, where the PF encounters large topographic features likely leads to increased nutrient flux to surface waters in these regions. The highest mean chlorophyll values associated with the PF occur where the front comes into contact with relatively shallow waters along the North Scotia Ridge and at Kerguelen Plateau. Iron input from sedimentary sources likely plays an important role in these regions.

Over seasonal timescales it appears likely that light-limitation prevents phytoplankton blooms at the PF during winter and spring months. PF blooms are observed most commonly during December when surface radiation peaks and mixed layer depths are rapidly shoaling. Even during December, when the light regime would seem to be favorable, PF blooms are largely restricted to regions where enhanced nutrient fluxes to surface waters due to frontal dynamics are likely. During late summer, nutrient limitation due to depletion of iron and possibly silicate largely prevent blooms at the PF. In the fall, deepening mixed layers would provide some relief from nutrient limitation but likely lead again to light-limitation of growth rates and the prevention of blooms.
© 2002 Elsevier Science B.V. All rights reserved.

Keywords: Phytoplankton; Southern Ocean; Mesoscale

1. Introduction

The Antarctic Polar Front (PF) is one of several strong fronts within the Antarctic Circumpolar Current (ACC) (Deacon, 1933; Mackintosh, 1946). Other circumpolar fronts within the ACC include the Sub-

antarctic Front (SAF) north of the PF, and the Southern Antarctic Circumpolar Current Front (SACCF) south of the PF (Orsi et al., 1995; Belkin and Gordon, 1996). There is a strong gradient in sea surface temperature (SST) across the PF, as it marks the surface transition between cold Antarctic surface water to the south and warmer, Subantarctic surface waters to the north. The PF is thus an important boundary in terms of air–sea fluxes and the heat and salt budgets of the ocean. The PF-associated current flows around Antarctica within the ACC as a meandering jet which exhibits considerable variability in the form of mesoscale meandering, eddy shedding, and ring formation (Mackintosh, 1946; Joyce et al., 1978; Moore et al., 1997, 1999a). Several studies have used satellite SST data to map the location of the PF (Legeckis, 1977; Moore et al., 1997; 1999a). The location and dynamics of the PF are strongly influenced by the bottom topography and the planetary potential vorticity field (Moore et al., 1997, 1999a).

Chlorophyll concentrations in the Southern Ocean are typically quite low despite high concentrations of the major nutrients nitrate and phosphate in surface waters (Tréguer and Jacques, 1992; Comiso et al., 1993; Banse, 1996; Banse and English, 1997; Moore et al., 2000; Moore and Abbott, 2000). The Southern Ocean is thus the largest of the High-Nitrate, Low-Chlorophyll (HNLC) regions (Martin, 1990). In recent years, substantial evidence has accumulated that the limited availability of the micronutrient iron limits growth rates, and in conjunction with loss processes maintains chlorophyll concentrations (and phytoplankton biomass) at relatively low levels within the Southern Ocean (Martin et al., 1990a,b; Helbling et al., 1991; de Baar et al., 1995; Van Leeuwe et al., 1997; Sedwick et al., 1997, 1999; Takeda, 1998; Boyd et al., 1999, 2000, 2001; Hutchins et al., 2001). Strong grazing pressure, light limitation, and silicon limitation of diatom growth have also been suggested to limit biomass accumulation in this region (Banse, 1996; Mitchell et al., 1991; Nelson and Smith, 1991; Boyd et al., 1999, 2001; Frank et al., 2000; Brown and Landry, 2001; Nelson et al., 2001; Hutchins et al., 2001).

As there is a strong seasonal cycle to solar radiation and mixed layer depths in this region, the factors listed above likely shift in their importance to the system over an annual cycle (Boyd et al., 1999; Abbott et al., 2000). During fall, winter, and early spring months, when mixed layers are deep, light limitation of phytoplankton growth rates is likely (Mitchell et al., 1991; Veth et al., 1997; Lancelot et al., 2000; Smith et al., 2000; Boyd et al., 2001). In addition, given the importance of iron for photoadaptation, iron-light co-limitation is also possible (Sunda and Huntsman, 1997; Boyd et al., 1999, 2000, 2001). Silicate concentrations at the PF and in waters to the south are high during winter/spring months, but may be strongly depleted during the growing season (Nelson et al., 2001) and may influence community composition and growth rates north of the PF all year (Hutchins et al., 2001). In addition, iron stress leads to an increased drawdown of silicate relative to nitrate (Takeda, 1998; Hutchins and Bruland, 1998). Thus, iron stress during spring/summer months may lead to silicate depletion in surface waters and Si-limitation later in the growing season (Boyd et al., 1999; De La Rocha et al., 2000). In a global simulation, Moore et al. (2002) found that this effect led to summertime Si-limitation over >4% of the world ocean. Silicate was strongly depleted during the Antarctic Environment and Southern Ocean Process Study (AESOPS) study to the extent that uptake rates were strongly limited at ambient concentrations (Nelson et al., 2001). Phytoplankton C/Chlorophyll ratios also likely evolve over seasonal timescales in response to changing surface irradiance and mixed layer depths.

Phytoplankton blooms associated with the PF are typically dominated by larger diatom species (Lutjeharms et al., 1985; Laubscher et al., 1993; Dafner and Mordosova, 1994; Jochem et al., 1995; de Baar et al., 1995; Smetacek et al., 1997; Brown and Landry, 2001). Smaller phytoplankton species experience strong grazing pressure by microzooplankton. Larger diatoms are often not subject to strong grazing pressure due to their size (Sherr and Sherr, 1994; Price et al., 1994; Selph et al., 2001; Gall et al., 2001; Zeldis, 2001). Predators of the larger diatoms typically have long reproductive times relative to the diatoms. Large diatoms in the Southern Ocean are grazed mainly by some of the larger microzooplankton, large copepods, krill, and salps. Krill and salp swarms can result in strong grazing pressure on diatoms, but their occurrence is quite patchy in space and time. Thus, most of the time it is likely that bottom-up control by light, iron limitation and/or silicon limitation prevents blooms of larger diatoms in the PF region.

The diatom-dominated blooms, which have resulted in the mesoscale iron addition experiments in the equatorial Pacific and Southern Ocean present evidence for this bottom-up control of the diatoms (Coale et al., 1996; Boyd et al., 2000). In this paper, we assume bottom-up control of diatom growth and biomass distribution in the vicinity of the PF. This is a simplification as biomass levels (chlorophyll concentrations) are a function of complex ecosystem dynamics that include phytoplankton growth rates combined with grazing and other loss processes (see Banse, 1992). It is diatom growth rates (not biomass) that are subject to bottom-up control, but the two are often linked to some extent. The assumption does not apply to smaller phytoplankton species, which experience heavy grazing pressure by the microzooplankton.

Phytoplankton blooms have been observed in the vicinity of the major Southern Ocean fronts (Lutjeharms et al., 1985; Tréguer and Jacques, 1992; Banse, 1996; Banse and English, 1997; Moore et al., 1999b; Moore and Abbott, 2000). A number of in situ meridional transects have found elevated phytoplankton biomass at the PF relative to surrounding waters (Allanson et al., 1981; Lutjeharms et al., 1985; Bidigare et al., 1986; Laubscher et al., 1993; Jochem et al., 1995; de Baar et al., 1995; Bathmann et al., 1997; Mengelt et al., 2001). While elevated chlorophyll concentrations have often been observed at the PF, little is known about the temporal or spatial distributions of these frontal-associated blooms. Here we analyze remotely sensed estimates of sea surface temperature and surface chlorophyll concentrations to map out the temporal and spatial variability of PF-associated phytoplankton blooms.

A detailed survey of the PF was conducted along 6°W in the spring of 1992 (de Baar et al., 1995, 1997; Smetacek et al., 1997; Bathmann et al., 1997). Several distinct diatom blooms were observed in the vicinity of the PF, this region within the PF and adjacent waters influenced by the PF including the surrounding eddy field was termed the Polar Frontal region (Smetacek et al., 1997). Three distinct PF-associated diatom blooms each dominated by different species developed over the 6-week study period, with chlorophyll concentrations exceeding 4 mg/m^3 (Smetacek et al., 1997). Higher dissolved iron concentrations observed within the PF were likely a contributing factor in bloom development (de Baar et al., 1995; Smetacek et al., 1997; Löscher et al., 1997; Lancelot et al., 2000). The PF and surrounding waters were also surveyed intensely along 170°W in the Pacific sector during AESOPS (Smith et al., 2000). During AESOPS, a bloom was observed within the PF and also at the SACCF during December 1997 (Moore et al., 1999b; Abbott et al., 2000, 2001; Mengelt et al., 2001; Barth et al., 2001). Moore et al. (1999b) presented Sea Viewing Wide Field of View Sensor (SeaWiFS) satellite imagery, which showed elevated chlorophyll within the PF across this whole region during December 1997 persisting in some areas into January 1998.

Several factors have been suggested to account for phytoplankton blooms at the PF. Lutjeharms et al. (1985) suggested cross-frontal mixing and increased vertical density stratification as two physical mechanisms that might lead to elevated phytoplankton biomass at the PF. However, Banse (1996) found little correlation between chlorophyll concentration and mixed layer depth (a function of density stratification) in this region. Cross-frontal mixing could be important if different factors were limiting phytoplankton growth north and south of the front. There is often a strong gradient in silicic acid concentrations across the PF, with low concentrations to the north, which may limit diatom growth (Tréguer and Jacques, 1992; Hutchins et al., 2001). Silica may also be limiting south of the PF during times of strong drawdown by the biota (Nelson et al., 2001; Mengelt et al., 2001). Several studies have suggested that higher levels of dissolved iron in surface waters at the PF led to elevated phytoplankton biomass (de Baar et al., 1995; Bathmann et al., 1997; Measures and Vink, 2001). Meander-induced upwelling or increased eddy mixing may lead to increased fluxes of nutrients (including micronutrients such as iron) into the surface layer, particularly where the ACC interacts with large topographic features (Moore et al., 1999b; Barth et al., 2001; Abbott et al., 2001).

Meandering of oceanic jets, such as the PF, leads to localized areas of upwelling and downwelling on spatial scales of 10–100 km through the conservation of potential vorticity. Vertical velocities associated with meanders can have rates of tens of meters per day (Pollard and Regier, 1992; Read et al., 1995; Pollard et al., 1995). Meander-induced upwelling can stimulate phytoplankton growth by increasing nutrient flux to surface waters and by improving the irradiance

regime for phytoplankton deeper in the water column (Flierl and Davis, 1993; Olson et al., 1994). Olson et al. (1994) argued that the secondary circulation and local eddy field associated with meanders play key roles in frontal biological enhancement. Dafner and Mordosova (1994) also stressed the role of eddy pumping as a source of nutrients. Meander-induced upwelling and eddy formation are likely intensified where Southern Ocean fronts interact with large topographic features (Moore et al., 1999a,b; Moore and Abbott, 2000). Barth et al. (2001) suggested that meander-induced upwelling of nutrients was likely the cause of the patterns of elevated chlorophyll in the PF observed during AESOPS from a towed Sea-Soar system equipped with CTD and bio-optical sensors. The SeaSoar surveys also revealed narrow bands of elevated chlorophyll (10–20 km wide) within distinct water masses that stretched for long distances along the PF (at least 120 km along front) (Barth et al., 2001). Abbott et al. (2001) found evidence for a biological impact due to meander-induced upwelling/ downwelling in data from bio-optical drifters released in the PF as part of AESOPS. During early spring the ratio of fluorescence/chlorophyll was positively correlated to vertical velocities estimated from clusters of drifters, which could result from an improved light regime and/or nutrient injection during upwelling events. Iron inputs from below and an improved irradiance regime due to shoaling would both alleviate iron stress (Sunda and Huntsman, 1997). Vertical velocities estimated from the near surface drifters reached 4 m/day within PF meanders, with significantly higher vertical velocities likely deeper in the water column (Abbott et al., 2001). Nelson et al. (2001) noted that by mid-summer waters north and south of the PF had silicic acid concentrations < 3 μM while values of 4–7 μM were measured in the vicinity of the PF. This suggests an increased flux of Si into surface waters at the PF relative to surrounding waters. Similarly Measures and Vink (2001) reported generally higher dissolved iron concentrations in the surface mixed layer at the two frontal zones associated with the PF and SACCF from transects along 170°W.

There have been a number of previous studies that examined satellite ocean color data from the Southern Ocean. Comiso et al. (1993) and Sullivan et al. (1993) examined pigment data for the whole Southern Ocean with the Coastal Zone Color Scanner (CZCS), which was in operation from 1978 to 1986. Banse (1996) compared CZCS data with in situ measurements over the Subantarctic Water Ring. Banse and English (1997) used CZCS data to study chlorophyll concentrations in the SW Pacific sector. Moore et al. (1999b) examined SeaWiFS data from the AESOPS study region during the 1997–1998 season. Moore and Abbott (2000) examined seasonal patterns within various ecological regions of the Southern Ocean during the 1997–1998 season with SeaWiFS data. One of the ecological regions studied was the Polar Frontal Region (PFR), which they defined as all areas within 1° latitude of the mean path of the PF as determined by Moore et al. (1999a). We adopt this definition for the Polar Frontal Region (PFR). This definition for the PFR is similar to that of Smetacek et al. (1997) but likely encompasses a somewhat larger area depending on hydrographic conditions.

In this study, we have used satellite sea surface temperature data to map the surface expression of the Antarctic Polar Front using methods developed previously (Moore et al., 1997, 1999a; see also below). These PF paths are then compared with satellite estimates of surface chlorophyll concentrations from SeaWiFS over weekly timescales. Our objectives were to quantify the spatial and temporal variability of phytoplankton blooms at the PF. Secondly, we wanted to gain insights into the mechanisms that lead to the formation of blooms at the PF.

2. Materials and methods

Satellite sea surface temperature (SST) data were used to map the location of the PF using methods described previously (Moore et al., 1997, 1999a). The SST data were obtained on a 9 km equal angle grid produced by the NOAA/NASA Pathfinder Project (Brown et al., 1993; Smith et al., 1996; Kilpatrick et al., 2001). Daily files (both ascending and descending passes) were composite-averaged (average of all valid data) to produce weekly maps of SST (interim Version 4.1 data). Briefly, our method for mapping the PF location is as follows (see Moore et al., 1997, 1999a for details). A "gradient map" is constructed which is a subset of the weekly SST map containing only those pixels within strong SST gradients (see Moore et al., 1997 for an example of SST image and the correspond-

ing gradient map). The strong SST gradient across the PF is used to subjectively digitize the poleward edge of the PF by examination of the weekly SST and gradient maps (Moore et al., 1997, 1999a).

Moore et al. (1999a) presented an analysis of a 7-year time series of weekly locations for the PF (or PF paths) covering the period 1987–1993. We have extended this time series of PF paths through mid-1999. Paths from the years 1997–1999 are compared with the satellite ocean color data to examine phytoplankton bloom dynamics at the PF. We have used the entire time series (>11 years) to calculate the mean location of the PF using the methods of Moore et al. (1999a).

Satellite ocean color estimates of surface chlorophyll concentrations are used to examine phytoplankton biomass and bloom dynamics in the vicinity of the PF. Daily level 3 standard mapped images of chlorophyll (Version 3) from SeaWiFS were obtained from the Goddard Space Flight Center (McClain et al., 1998). The SeaWiFS data used in this study cover the period from October 1997 to March 1999. Daily files were composite-averaged to produce weekly maps of surface chlorophyll concentration on a global 9 km equal angle grid.

The weekly SST and chlorophyll maps contain large areas with no valid data due to the extensive cloud cover over the Southern Ocean. Thus, only a portion of the PF is visible in any weekly image. Since sea surface temperature is collected at night as well as during the day SST coverage is generally better than the ocean color data coverage, which can only be collected during daylight hours. In this study, we use all weekly SST and chlorophyll maps during the October–March growing season for the years 1997–1998 and 1998–1999.

We calculate mean chlorophyll concentrations within the PF and within a swath on either side (poleward and equatorward) of the front. To be considered within the PF, pixels had to be within the strong gradient of SST across the front (retained in our gradient maps). We calculate mean chlorophyll concentrations at right angles to the PF path over a swath approximately 60 km equatorward and poleward of the front. The actual width of these swaths varied somewhat with latitude (as pixel area does) and with the orientation of the PF (i.e. PF current flowing west, northwest, etc.). Directional orientation for averaging chlorophyll concentrations within and on either side of

the front was determined at each point along the PF paths by examining the direction of the next point along the path in the downstream direction. Thus, if the next point was to the east at the exact same latitude, data was averaged in the north–south orientation.

3. Results

Displayed in Fig. 1 are the individual PF paths used in this study (thin lines) and the mean position of the PF calculated from the full time series of PF paths (1987–1999, thick black line). The mean path is nearly identical to the mean path of Moore et al. (1999a), which was based on the 1987–1993 data. It can be seen from Fig. 1 that there were large spatial variations in the number of paths mapped. Fewer paths are seen above the deep ocean basins (~ 130–90°W, ~ 50–70°E, ~ 110–140°E), while the highest number of paths digitized are in the Drake Passage/Scotia Sea region (90–35°W), and to a lesser extent downstream of Kerguelen Plateau (75–100°E), and along the Pacific–Antarctic Ridge (~ 180–140°W). These spatial patterns are similar to those found previously and are driven largely by the intensity of the SST gradient and to a lesser extent by regional cloud cover patterns (Moore et al., 1999a). Above the deep ocean basins, the SST gradient associated with the PF is weakened to the extent that it is frequently not distinguishable from the background north–south temperature gradient in our analysis (Moore et al., 1999a). Thus, few PF paths are mapped in these regions. In contrast, the temperature gradient is intensified in the vicinity of large topographic features (Moore et al., 1997, 1999a).

We calculated mean chlorophyll concentrations within the PF and along swaths to either side (poleward and equatorward of the front). There was a strong seasonal cycle in these mean chlorophyll values, with peak values during December in phase with the seasonal radiation cycle (Fig. 2). In many areas, mixed layer depth shoals in December and iron concentrations are still likely to be relatively high, retaining the wintertime, deep-mixing signal. Mean chlorophyll concentrations were quite low prior to November and after January. Strong light-limitation of phytoplankton growth in early spring when mixed layers are deep is likely (Veth et al., 1997; Abbott et al., 2000; Lancelot et al., 2000; Smith et al., 2000; Boyd et al.,
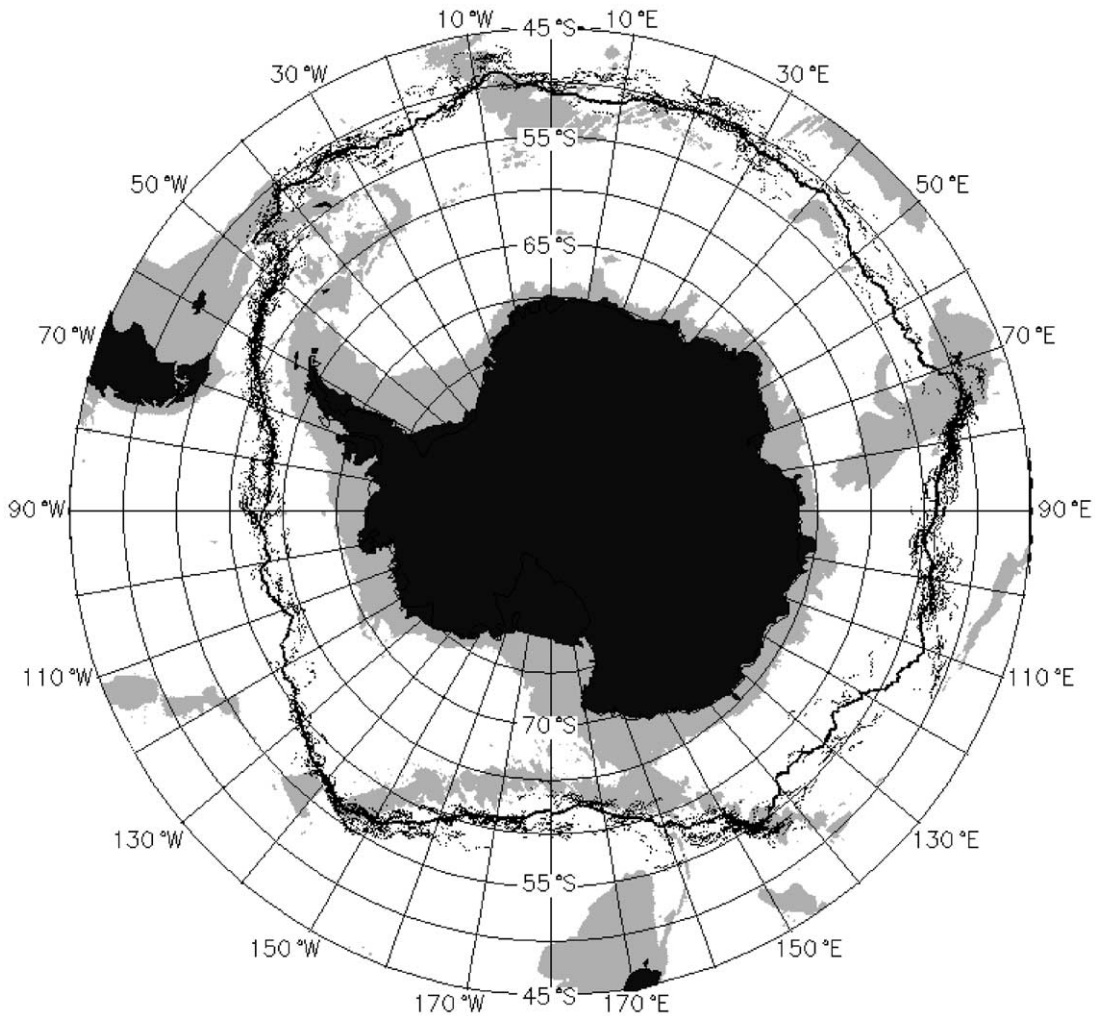
Fig. 1. Displayed are the long-term, mean position of the Antarctic Polar Front (thick black line) and the weekly positions used in this study from the October–March period for the 1997–1998 and 1998–1999 seasons. Gray shaded areas indicate ocean depth < 3000 m (bathymetry from Smith and Sandwell, 1994).

2001). During fall, light levels decline, mixed layers deepen and nutrients (particularly Fe and silicate) are at their seasonally depleted minimum values. Only during December were mean chlorophyll concentrations within the PF higher than in surrounding waters, when averaged over the whole Southern Ocean (Fig. 2). A number of blooms within the PF were also observed during January in the weekly images, and only rarely seen in other months.

During AESOPS mixed layers were deep (>100 m) during November then shoaled to less than 40 m during the December cruise (Smith et al., 2000). This initiated phytoplankton blooms across the region (Moore et al., 1999b; Abbott et al., 2000; Smith et al., 2000). While mixed layers remained relatively shallow during January, chlorophyll concentrations declined sharply at the PF, likely due to increasing iron and Si limitation (Abbott et al., 2000; Nelson et al., 2001; Measures and Vink, 2001). Boyd et al. (2001) found deep mixed layers at the PF during late summer 1998 in the Australian sector and suggested co-limitation by iron and light.
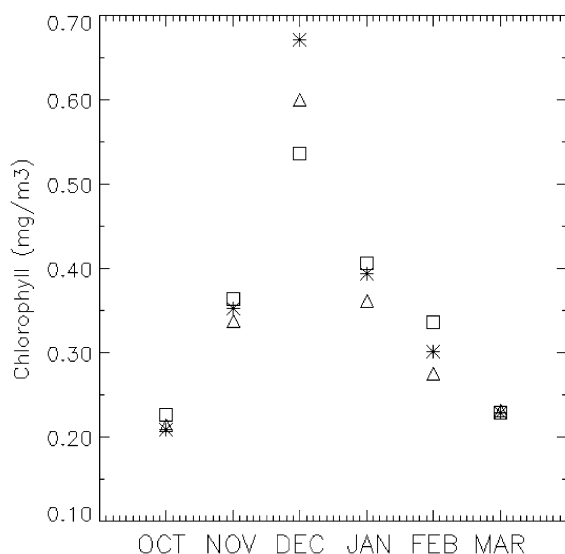
Fig. 2. Mean monthly chlorophyll concentrations averaged within the PF (asterisks) and within ~ 60 km swaths equatorward (triangles) and poleward (squares) of the PF (see text for details).

The seasonal pattern evident in Fig. 2 is similar to the pattern for the whole PFR in Moore and Abbott (2000). However, the December values (Fig. 2) are much higher than the December mean value for the PFR of 0.43 mg/m^3 calculated by Moore and Abbott (2000). The PFR contains substantial areas of open ocean by definition due to its relatively broad meridional extent (2° latitude) and because meanders of the front mean that using the mean position to define the PFR only roughly captures this region. Thus, the averages of Moore and Abbott (2000) do not capture well the PF blooms evident during December in Fig. 2. Values in Fig. 2 are also slightly higher than those calculated for the entire PFR by Moore and Abbott (2000) during the months of November, January, and February. This suggests that PF blooms are sporadic during these months and only weakly influence circumpolar mean PFR values.

There is considerable spatial variability in mean chlorophyll concentrations in the vicinity of the PF (Fig. 3). Displayed in Fig. 3 are mean chlorophyll concentrations over the October–March period (both the 1997–1998 and 1998–1999 seasons) within 5° longitudinal bins for regions within the PF and along swaths to the north and south. Also shown is the mean ocean depth over a 90-km-wide swath centered on our

mean PF path. Lowest chlorophyll concentrations are above the deep ocean basins (~ 125–90°W, ~ 55–65°E, and ~ 115–140°E, Fig. 3). Elevated chlorophyll concentrations are seen in several regions. The highest values are in the vicinity of Kerguelen Plateau (70–80°E), and downstream of the Scotia Sea (~ 45–30°W). Moderately high chlorophyll values are also seen along the Pacific–Antarctic Ridge (~ 170°E–150°W), and along the Mid-Atlantic Ridge (~ 15–35°E) (Fig. 3). In all of these areas, the PF is interacting with large topographic features (Moore et al., 1997, 1999a). The SST gradient associated with the PF is intensified in these regions and mesoscale meandering is also increased (at spatial scales < 100 km; Moore et al., 1999a). Approximately, 43% of these bins have mean chlorophyll concentrations in the PF region greater than 0.3 mg/m^3, and 12.5% of the bins exceed 0.4 mg/m^3.

There is also considerable regional variability if we compare chlorophyll concentrations within, equatorward and poleward of the PF (Fig. 3). Mean values within the PF are higher than in adjacent waters in the southwest Pacific, in the vicinity of Kerguelen Plateau and areas just downstream, and where the PF is forced into shallower waters entering Drake Passage (~ 90–70°W) (Fig. 3, also compare with the detailed bathymetry and PF location map of Moore et al., 1999a). In the southeast Pacific and within Drake Passage, mean chlorophyll concentrations poleward of the PF are much lower than within the PF and areas equatorward. Low chlorophyll concentrations south of the PF in Drake Passage have been observed previously (Comiso et al., 1993; Moore and Abbott, 2000). This low-chlorophyll region appears to be bounded by the PF (to the north) and the SACCF (to the south) (see following section and Fig. 3 of Moore and Abbott, 2000). Chlorophyll concentrations poleward of the PF are higher than those within and north of the PF in the Atlantic sector downstream of the Scotia Sea (~ 30–5°W), from 20–30°E, and in some of the bins between 140° and 180°E, most notably from ~ 150° to 160°E and ~ 170° to 175°E (Fig. 3). In this last region between 160° and 180°E, the seasonal ice cover extends into the PFR (Moore et al., 2000; Moore and Abbott, 2000). Thus, the elevated chlorophyll south of the PF is likely due to ice edge blooms.

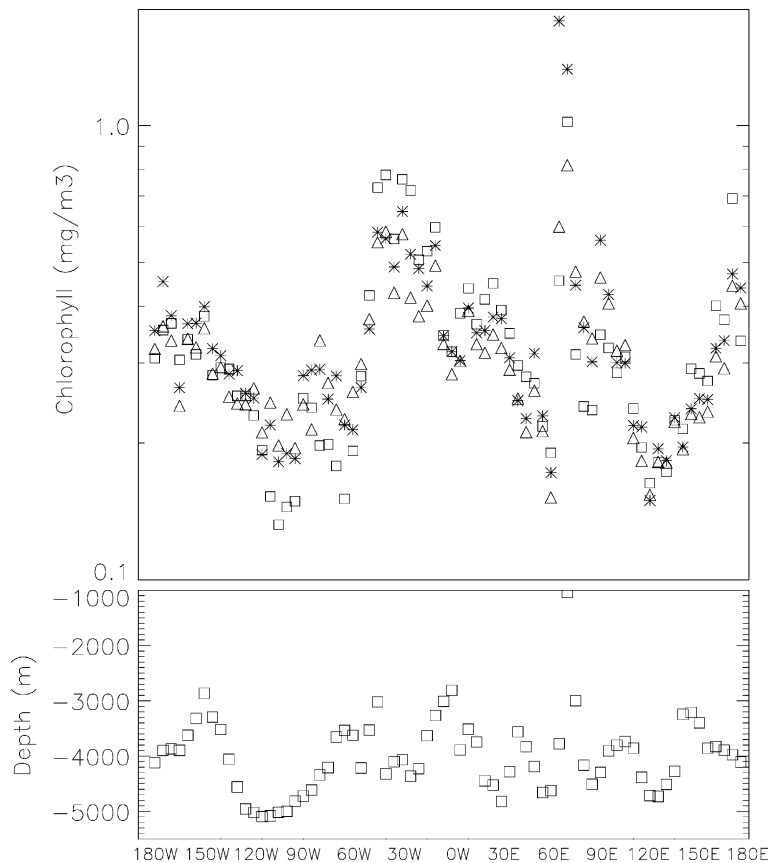Topography has a strong influence on the physics and biology of the PF. The PF can regularly come in

Fig. 3. Mean chlorophyll concentrations within the PF (asterisks) and within ~ 60 km swaths equatorward (triangles) and poleward (squares) of the PF averaged over 5° longitudinal bins from the October–March period for the 1997–1998 and 1998–1999 seasons. Also shown is the mean ocean depth along the mean path of the PF (bathymetry from Smith and Sandwell, 1994).

contact with relatively shallow waters (< 500 m) in two regions of the Southern Ocean, along the North Scotia Ridge, and at the Kerguelen Plateau, both regions of generally elevated chlorophyll levels in the vicinity of the PF (Fig. 3). Large plumes of elevated chlorophyll concentrations frequently extend for hundreds of kilometers downstream of both of these topographic features (Moore and Abbott, 2000). Shallow waters can be an important source of iron to surface waters. Iron concentrations in coastal and shallow waters can be an order of magnitude higher than in open ocean waters (Martin et al., 1990a,b; Nolting et al., 1991; Johnson et al., 1999; Blain et al., 2001). Comiso et al. (1993) found an inverse correlation between ocean depth and chlorophyll concentrations over the entire Southern Ocean. Blain et al.

(2001) investigated the Kerguelen Islands and surrounding Kerguelen Plateau as a source of dissolved iron for downstream waters. They found very high iron concentrations >10 nM near the islands. Offshore waters had lower concentrations, but still significantly higher than typically measured Southern Ocean values (Blain et al., 2001). They suggested that lithogenic inputs from the islands as well as inputs of iron from the shelf and the plateau are important iron sources for surrounding (and downstream) waters. Deep winter mixing can reach shelf/sediment iron sources in the Southern Ocean resulting in substantial re-suspension of sediments. Entrainment through current motions and turbulent mixing are also likely.

Fig. 4 displays the topography and mean surface chlorophyll concentrations in the northern Scotia Sea
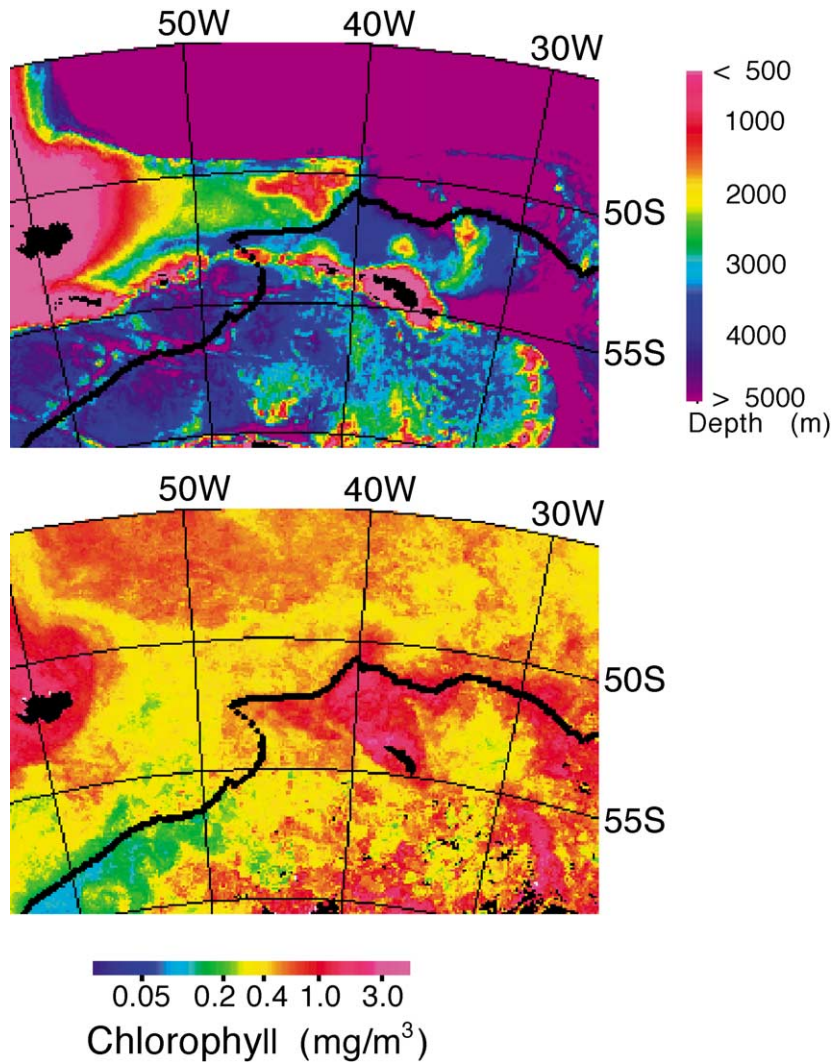
Fig. 4. Bathymetry and mean chlorophyll concentrations (during December and January) are shown in relation to the mean position of the Antarctic Polar Front in the Northern Scotia Sea region. Mean chlorophyll calculated by averaging weekly composites from December and January during the 1997–1998 and 1998–1999 seasons. Bathymetry data is from Smith and Sandwell (1994).

region in relation to the mean position of the PF. Mean chlorophyll was calculated by averaging the weekly images from December and January. The PF typically crosses the North Scotia Ridge at the Shag Rock Passage (∼ 47–49°W, 53.3°S) (Peterson and Whitworth, 1989; see also Moore et al., 1997). This gap marks the only location on the North Scotia Ridge where ocean depth >2000 m (Fig. 4). West of Shag Rock Passage on the North Scotia Ridge lies a small cluster of islands known as Shag Rocks (∼ 46.6°W,

53°S). The PF closely follows the southern flank of Ewing Bank after crossing the North Scotia Ridge (Moore et al., 1997, 1999a; Trathan et al., 1997, 2000). A large region of elevated chlorophyll can be seen beginning at the North Scotia Ridge and bounded to the west and north by the PF (Fig. 4).

Highest chlorophyll concentrations are seen in shallow waters near South Georgia Island at ∼ 38°W, 54°S (Fig. 4). As ACC waters move north across the ridge it is likely that this region of high chlorophyll is

initiated because iron and possibly other nutrients (particularly Si) are injected into surface waters. Injection of silicate would likely be important only later in the season after initially high springtime concentrations (due to deep winter mixing) had been depleted. This large region of elevated chlorophyll accounts for the higher chlorophyll concentrations seen south of the PF from 45° to 35°W in Fig. 3. A similar topography-related elevation of chlorophyll levels is apparent along the arc that forms the South Sandwich Islands (north–south line of shallow bathymetry between ~ 29° and 27°W from ~ 56° to 59°S, Fig. 4). High chlorophyll concentrations are also observed above the Patagonian shelf in the shallow water region around the Malvinas (Falkland) islands. The Subantarctic Front (SAF) moves to the north just east of these islands closely following bathymetric contours. The SAF here acts as an efficient boundary separating high-chlorophyll waters above the shelf from low-chlorophyll waters to the east. Note also in Fig. 4 the very low chlorophyll concentrations south of the PF within Drake Passage (west of ~ 55°W).

Next we examine weekly images of phytoplankton blooms in the vicinity of the Antarctic Polar Front. Phytoplankton blooms at the PF are often smaller in spatial extent than the regions over which chlorophyll was averaged for Figs. 2 and 3. For example, elevated chlorophyll is often observed within a narrow band that occupies only a portion of the strong SST gradient of the PF. In some cases, the PF merely acts as a boundary between different water masses north and south of the front. In these cases, chlorophyll concentrations within the front are intermediate between those equatorward and poleward. These two images (Figs. 5 and 6) were chosen to illustrate common patterns in chlorophyll distributions at the front, and because they had relatively little missing data due to persistent cloud cover. The missing data due to cloud cover still seen in these images illustrates how severe the cloud cover problem is in this region.

In the figures that follow, our weekly PF path (which marks the poleward edge of the PF) is shown in white overlain on the weekly chlorophyll and SST gradient maps. Insets also show mean chlorophyll and SST at the PF averaged over 1° longitudinal bands for areas within and to either side of the front. The SST and chlorophyll data are from the same week in each case, but depending on cloud cover and satellite orbital variations, measurements may not be from the same day, and in fact could be separated by up to 1 week. The PF can shift its location substantially in 1 week, on average by 22 km between successive weekly SST images (Moore et al., 1999a).

Weekly images of chlorophyll and SST gradients from the week beginning December 3, 1997 are shown in Fig. 5. A large phytoplankton bloom is evident from 180° to 172°W over a broad latitudinal range. This bloom is likely associated with retreating sea ice cover in this region (Moore et al., 1999b; Moore and Abbott, 2000). Melting sea ice can stimulate phytoplankton blooms by shallowing the mixed layer and thus improving the irradiance regime (Smith and Nelson, 1986) and by adding dissolved iron to surface waters (Martin, 1990; Sedwick et al., 2000). A strong phytoplankton bloom within the PF is apparent stretching nearly continuously from the ice edge bloom to ~ 138°W where our PF path ends (Fig. 5). This is the PF bloom that was observed in situ along 170°W during AESOPS and in the composite satellite images of Moore et al. (1999b).

Note that although the elevated chlorophyll and strong SST gradient are generally co-located, in some areas the elevated chlorophyll band is wider than the strong temperature gradient, while in other areas it is narrower. This occurs for a couple of reasons. First our definition of a strong SST gradient is a subjective one and local mesoscale processes can shift the edge of the strong gradient region. Secondly, as noted by Barth et al. (2001), often elevated chlorophyll occurs as a narrow along-front band, which does not occupy the entire frontal temperature gradient. These patterns will tend to blur the mean values calculated for within, south, and north of the PF shown in Figs. 2 and 3, and as insets to Fig. 5. This banded or step-like structure across the PF has been noted previously in sea surface temperature data (Belkin, 1988).

Fig. 5. Weekly image of chlorophyll concentration and the corresponding sea surface temperature gradient map for the week beginning December 3, 1997 (see text for details). The poleward edge of the Antarctic Polar Front is overlain in white on both images. Insets show mean chlorophyll and sea surface temperature within the PF (asterisks) and within ~ 60 km swaths equatorward (triangles) and poleward (squares) of the PF from the weekly images, calculated within 1° longitudinal bins.
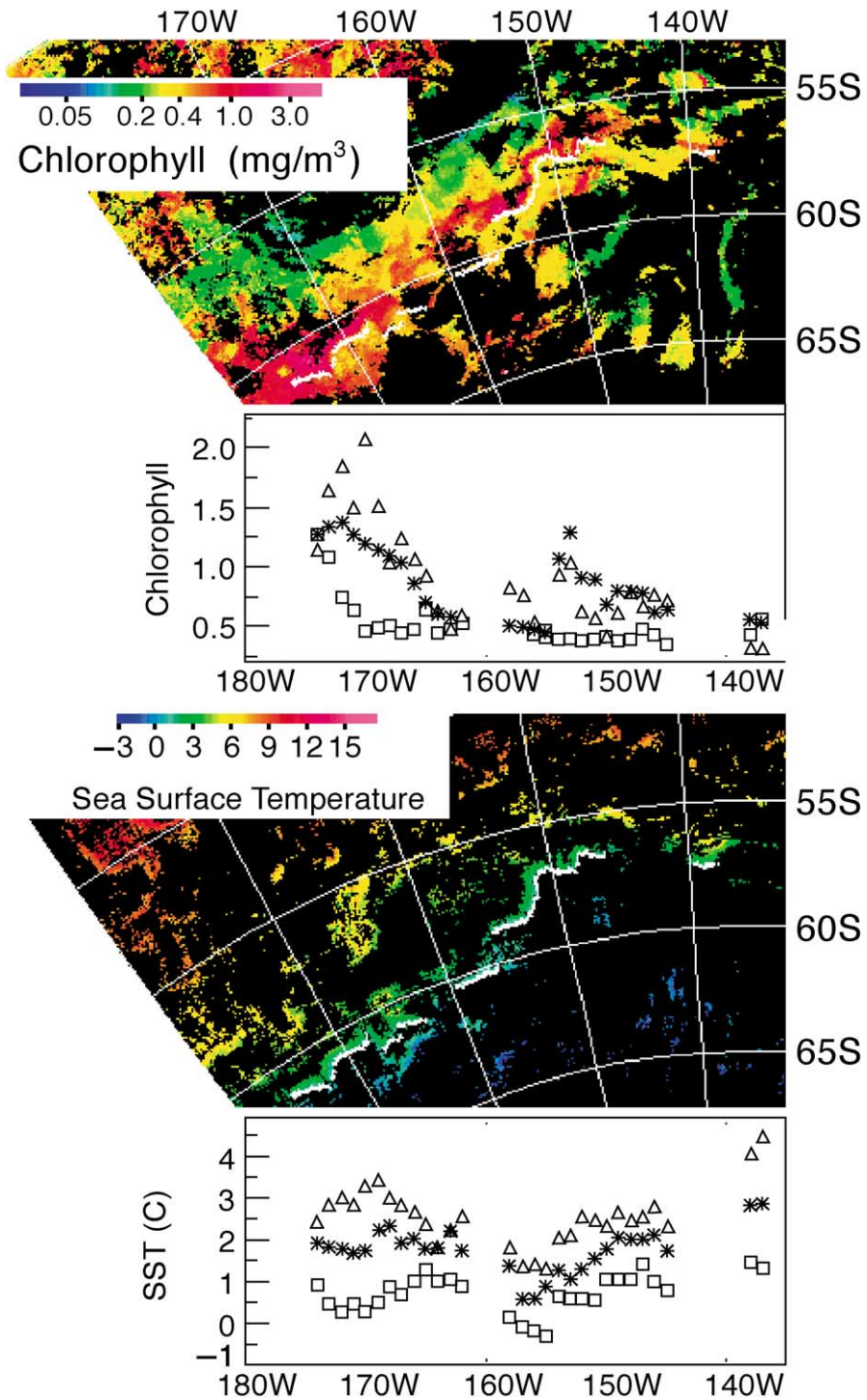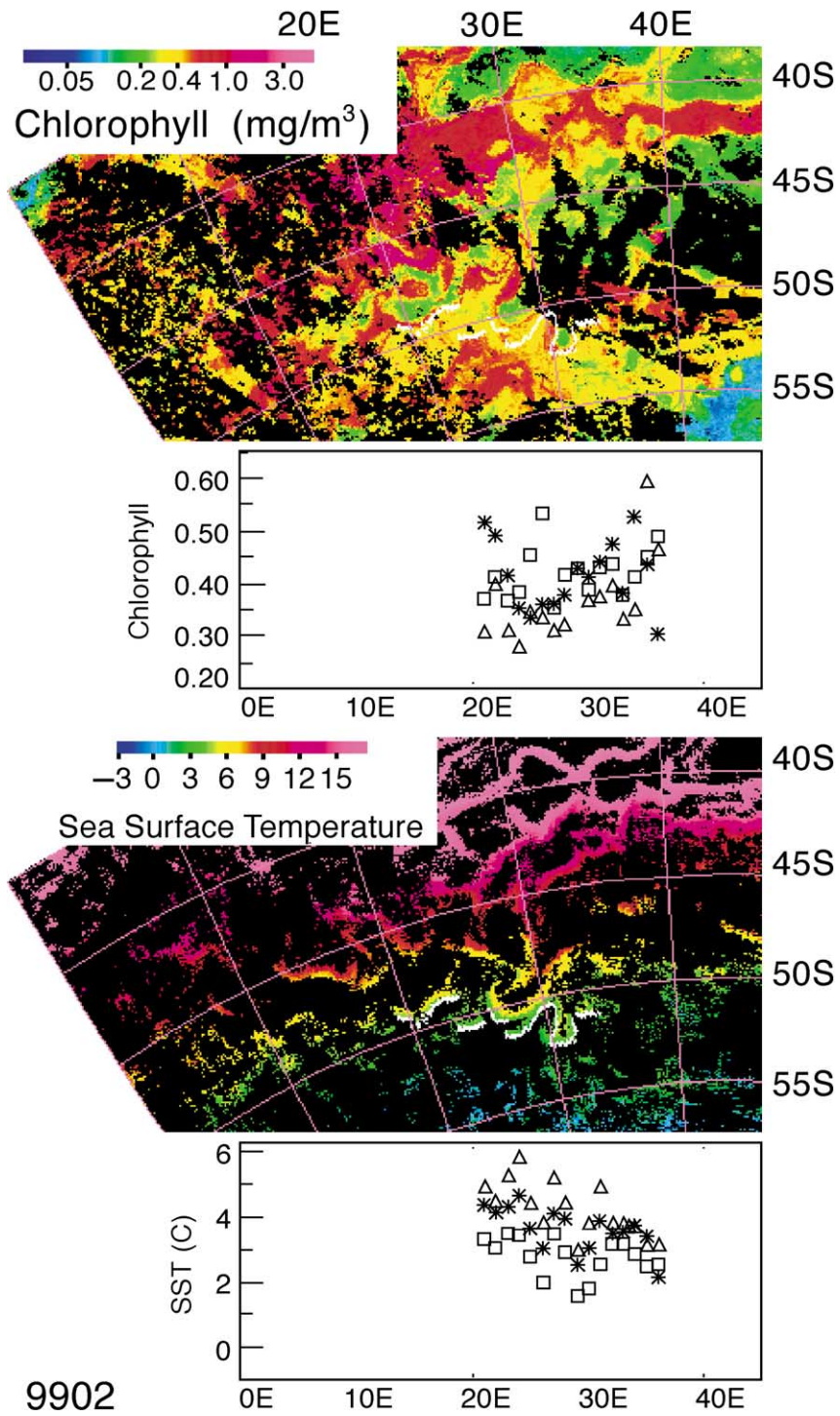
Examining the insets of chlorophyll and SST averaged within 1° longitudinal bands it can be seen that as expected SST is warmer north of the front and colder south of the front (Fig. 5). Chlorophyll concentration is higher north of the PF than within the front or to the south for the region 175–165°W, and values within the front are higher than surrounding waters from 155° to 148°W (Fig. 5). Along 170°W, mean chlorophyll values within the PF are slightly more than 1.0 mg/m^3, which is in excellent agreement with estimates from bio-optical moorings at the PF for this time period (Abbott et al., 2000).

In this region, the PF is following the northern flank of the Pacific–Antarctic Ridge (see Fig. 1 and Moore et al., 1999a,b; Abbott et al., 2001). The sharp northward bend at ~ 152°W is located where the PF is forced into shallower waters prior to crossing the Pacific–Antarctic Ridge (Moore et al., 1999b). Abbott et al. (2001) found evidence for upwelling in a poleward meander and downwelling within an equatorward meander in this region by analyzing clusters of surface drifters. Evidence for these same patterns can be seen in Fig. 5. The area of elevated chlorophyll expands in the poleward meander between ~ 156° and 153°W, then narrows as the front turns northward and enters an equatorward meander from ~ 152° to 150°W (Fig. 5). These patterns of upwelling and downwelling are what one would expect within a meandering jet (Olson et al., 1994). PF blooms were most commonly observed along the Pacific–Antarctic Ridge (Fig. 3). Elevated chlorophyll concentrations along the Pacific–Antarctic and Southeast Indian Ridges are also readily apparent in the monthly SeaWiFS composites of Moore and Abbott (2000), and were also observed with the CZCS (Comiso et al., 1993; Sullivan et al., 1993).

Mean chlorophyll and SST gradient maps for the region from 0° to 45°E for the week beginning January 8, 1999 are shown in Fig. 6. In this image, some elevated chlorophyll in the vicinity of the PF is apparent between 10° and 30°E along ~ 49°S. A very narrow band of elevated chlorophyll within the

PF is seen between ~ 19° and 25°E. Note that this elevated chlorophyll occupies only a portion of the strong SST gradient, similar to the pattern described by Barth et al. (2001) in the Pacific sector during AESOPS. A narrow band of elevated chlorophyll within the PF is also seen in the southward bend at ~ 26–30°E (Fig. 6). A wide band of elevated chlorophyll south of the PF for approximately 3° of latitude (between 20° and 30°E) is situated directly above the Mid-Atlantic Ridge. The PF forms the northern boundary of this region from ~ 23° to 25°E where chlorophyll values south of the PF are higher than within or to the north of the front (see chlorophyll inset Fig. 6). Chlorophyll values within the front are higher than surrounding waters from 20° to 23°E and from 28° to 33°E (Fig. 6). Again waters equatorward of the PF are generally warmer than waters to the south. The chlorophyll and SST (inset) averages are questionable east of ~ 32°E where tight meanders and possibly a warm core ring result in points south of the front being averaged into the equatorward of the front region. This strong meso-scale variability is another factor that can blur the distinct regions averaged in Figs. 2 and 3. Elevated chlorophyll can also be seen farther north associated with the Subantarctic and Subtropical fronts with a strong correlation apparent between regions of elevated chlorophyll and frontal locations. The PF turns sharply southwards at ~ 30–31°E.

Satellite altimetry and drifter studies have found high eddy variability in the region near 30°E (Daniault and Ménard, 1985; Sandwell and Zhang, 1989; Chelton et al., 1990; Morrow et al., 1994). The PF undergoes intense meandering in this region (Moore et al., 1999a) and regularly spawns warm core rings (Gouretski and Danilov, 1993, 1994). Moore et al. (1999a) noted interactions between the SAF and the PF in this region. Such interaction is apparent in Fig. 6. A warmer strong SST gradient (the SAF) north of the PF also turns southward at ~ 31°E and comes in contact with the PF. The southward bend in both fronts is a persistent feature and is driven largely by the topography (Moore et al., 1999a).

Fig. 6. Weekly image of chlorophyll concentration and the corresponding sea surface temperature gradient map for the week beginning January 8, 1999 (see text for details). The poleward edge of the Antarctic Polar Front is overlain in white on both images. Insets show mean chlorophyll and sea surface temperature within the PF (asterisks) and within ~ 60 km swaths equatorward (triangles) and poleward (squares) of the PF from the weekly images, calculated within 1° longitudinal bins.

4. Discussion

Phytoplankton blooms at the Antarctic Polar Front are unevenly distributed through space and time. PF blooms where chlorophyll concentrations within the front exceed those of surrounding waters occur most frequently during the month of December (Fig. 2). December marks the peak in surface solar radiation and is a time of rapidly warming sea surface temperatures within the Southern Ocean and frequently a rapid shoaling of mixed layer depths (for the seasonal SST cycle at the PF, see Moore et al., 1999a). In addition, nutrients replenished in surface waters by deep winter mixing are likely still near their seasonal maximum. Maximum chlorophyll concentrations are seen during December over most of the Southern Ocean, although maximum values within the Seasonal Ice Zone occur during January (Moore and Abbott, 2000). Thus, the seasonal pattern observed at the PF is consistent with what is a relatively weak spring bloom in the Southern Ocean.

There is a large degree of spatial variability in chlorophyll concentrations associated with the PF (Fig. 3). Often elevated chlorophyll appears as a narrow band that occupies only a portion of the SST gradient across the PF (Figs. 5 and 6). The highest mean chlorophyll concentrations are observed where the PF comes into contact with relatively shallow waters (<500 m) along the North Scotia Ridge and at Kerguelen Plateau. The elevated chlorophyll signal from these shallow regions persists for hundreds of km downstream and over much of the growing season. It is likely that these shelf areas are a strong source of dissolved iron, which in turn stimulates the growth and blooming of larger diatom species. This iron input must be retained for some time in near surface/surface waters either in biomass, detrital, or dissolved form.

PF blooms were also frequently observed in other regions where the PF interacts with large topographic features including along the Southeast Indian and Pacific–Antarctic Ridges, through Drake Passage, and along the Mid-Atlantic Ridge. Ocean depths in these regions are typically >2000 m so a sedimentary source of iron for surface waters is unlikely. Iron added from the sediments would likely be removed by scavenging long before it could mix/upwell into surface waters. It is more likely that mesoscale physical

processes, which occur where the PF encounters these large topographic features, lead to increased nutrient injection from sub-surface to surface waters (Moore et al., 1999b).

Mesoscale meandering of the PF is intensified where the PF crosses large topographic features and for several hundred kilometers downstream (Moore et al., 1999a). This meandering leads to localized areas of upwelling which can stimulate phytoplankton growth through nutrient injection to the euphotic zone and by moving phytoplankton deep in the water column to higher light levels closer to the surface (Flierl and Davis, 1993; Olson et al., 1994; Moore et al., 1999b; Moore and Abbott, 2000; Barth et al., 2001; Abbott et al., 2001). Such intense meandering also increases eddy shedding/mixing, which increases the rate at which sub-surface nutrients enter surface waters (Olson et al., 1994; Abbott et al., 2001).

The large changes in ocean depth where the ACC crosses large topographic features inputs large amounts of relative vorticity to the water column. This relative vorticity is likely dissipated at least partly through increased eddy actions, which would increase nutrient flux to surface waters (Moore et al., 1999b). This vorticity/eddy mixing effect would apply to the PF and to open ocean ACC waters. This process may partially account for the broad regions of elevated chlorophyll seen above large topographic features in this study and in Moore and Abbott (2000).

These phytoplankton blooms, which seem to be responding to inputs of nutrients to the surface layer, are most likely responding to inputs of dissolved iron and silicic acid from sub-surface waters. Particularly north of the PF, Si limitation of diatom growth is likely (Tréguer and Jacques, 1992; Boyd et al., 1999). Silicate depletion can also lead to Si limitation south of the PF later in the season (Nelson et al., 2001). Recent studies of the PF region along 170°W as part of AESOPS indicates that iron and Si can be depleted in the upper portions of the water column north and south of the PF to depths of several hundred meters (Nelson et al., 2001; Measures and Vink, 2001). This sub-surface depletion may be reflected in our results. While PF blooms were observed with chlorophyll concentrations significantly elevated relative to surrounding waters, absolute concentrations within the blooms tended to remain at moderate levels (typically <1.5 mg/m^3, and often <1.0 mg/m^3). Thus, despite the increased

nutrient inputs to surface waters, accumulation of phytoplankton biomass is likely still limited by iron and/or Si availability, particularly later in the growing season. Other factors such as light limitation and grazing pressure are likely significant at times as well.

Recent chemostat culture work with natural assemblages of Southern Ocean phytoplankton may provide insight into the observed PF blooms. Experiments using natural phytoplankton assemblages were conducted at different rates of dilution and with typically low Southern Ocean iron concentrations (Hutchins et al., 2002, in preparation). Using a low dilution rate (low nutrient flux rate into the chemostat) the resulting assemblage was dominated by smaller phytoplankton species with relatively low chlorophyll concentrations (similar to what is observed in situ over much of the Southern Ocean). However, at faster dilution rates (faster input rates, but still relatively low iron concentrations) the species composition shifted toward domination by larger, fast growing diatoms, with a higher chlorophyll concentration maintained. As meanders of the PF can persist for weeks one can envision a localized, meander-induced upwelling as a point source of increased rate flux of subsurface nutrients into surface waters as the input to the "chemostat" with subduction downstream leading to increased losses of phytoplankton from surface waters. Areas of increased eddy mixing induced by the topography could function in the same manner. Thus, the mesoscale physical processes may increase nutrient flux to surface waters and select for larger diatoms, leading to elevated chlorophyll concentrations.

In summary, the monthly mean data presented in Fig. 2 illustrates that phytoplankton blooms within the PF are largely restricted to the month of December. We did observe some blooms during January, but very few during other months. Prior to December light limitation of growth rates likely prevents biomass accumulation due to deep mixed layers and lower surface radiation (Mitchell et al., 1991; Veth et al., 1997; Abbott et al., 2000; Lancelot et al., 2000; Smith et al., 2000). As mixed layers shoal during late spring, blooms are initiated particularly in areas where frontal dynamics increase nutrient flux to surface waters (see Fig. 3 and discussion above). By mid to late summer, iron and in some instances silicate have been depleted to levels that strongly limit growth rates and prevent bloom occurrence (Abbott et al., 2000; Measures and Vink, 2001;

Nelson et al., 2001; Hutchins et al., 2001). Later in the season, light-limitation likely becomes an important factor in controlling phytoplankton blooms in the PF region as mixed layers deepen and solar radiation declines (Boyd et al., 2001).

Future analyses of satellite and in situ data combined with modeling studies can improve our understanding of phytoplankton bloom dynamics at the Antarctic Polar Front. As a longer time series of satellite ocean color data becomes available, further analysis of co-temporal chlorophyll and sea surface temperature images, and incorporation of wind data from satellite scatterometer missions will enable more detailed studies of bloom dynamics at the PF and at other Southern Ocean fronts. However, many aspects of ecosystem dynamics cannot be measured using remote sensing data alone. Linking the new wealth of remote sensing data with in situ observations and ecosystem models will be critical for future progress.

Acknowledgements

References

Abbott, M.R., Richman, J.G., Bartlett, J.S., 2000. The spring bloom in the Antarctic Polar Frontal Zone as observed from a mesoscale array of bio-optical sensors. Deep-Sea Res., Part II 47, 3285–3314.

Abbott, M.R., Richman, J.G., Bartlett, J.S., Barksdale, B.S., 2001. Meanders in the Antarctic Polar Frontal Zone and their impact on phytoplankton. Deep-Sea Res., Part II 48, 3891–3912.

Allanson, B.R., Hart, R.C., Lutjeharms, J.R.E., 1981. Observations on the nutrients, chlorophyll, and primary production of the Southern Ocean south of Africa. S. Afr. J. Antarct. Res. 10/11, 3–14.

Banse, K., 1992. Grazing, temporal changes of phytoplankton concentrations, and the microbial loop in the open sea. In: Falkowski, P.G., Woodhead, A.D. (Eds.), Primary Productivity and Biogeochemical Cycles in the Sea. Plenum, New York, pp. 409–440.

Banse, K., 1996. Low seasonality of low concentrations of surface chlorophyll in the Subantarctic water ring: underwater irradiance, iron, or grazing? Prog. Oceanogr. 37, 241–291.

Banse, K., English, D.C., 1997. Near-surface phytoplankton pigment from the Coastal Zone Color Scanner in the Subantarctic region southeast of New Zealand. Mar. Ecol. Prog. Ser. 156, 51–66.

Barth, J.A., Cowles, T.J., Pierce, S.D., 2001. Mesoscale physical and bio-optical structure of the Antarctic Polar Front near 170°W during spring. J. Geophys. Res. 106, 13879–13902.

Bathmann, U.V., Scharek, R., Klaas, C., Dubischar, C.D., Smetacek, V., 1997. Spring development of phytoplankton biomass and composition in major water masses of the Atlantic sector of the Southern Ocean. Deep-Sea Res., Part II 44, 51–67.

Belkin, I.M., 1988. Main hydrological features of the central South Pacific. In: Vinogradov, M.E., Flint, M.V. (Eds.), Ecosystems of the Subantarctic Zone of the Pacific Ocean. Nauka, Moscow, pp. 21–28. In Russian, English translation: Pacific Subantarctic Ecosystems, New Zealand Translation Centre, Wellington 1997, pp. 12–17.

Belkin, I.M., Gordon, A.L., 1996. Southern Ocean fronts from the Greenwich meridian to Tasmania. J. Geophys. Res. 101, 3675–3696.

Bidigare, R.R., Frank, T.J., Zastrow, C., Brooks, J.M., 1986. The distribution of algal chlorophylls and their degradation products in the Southern Ocean. Deep-Sea Res., Part I 33, 923–937.

Blain, S., Tréguer, P., Belviso, S., Bucciarelli, E., Denis, M., Desabre, S., Fiala, M., Jézéquel, V.M., Le Fèvre, J., Mayzaud, P., Marty, J.C., Razouls, S., 2001. A biogeochemical study of the island mass effect in the context of the iron hypothesis: Kerguelen Islands, Southern Ocean. Deep-Sea Res., Part I 48, 163–187.

Boyd, P., LaRoche, J., Gall, M., Frew, R., McKay, R.M.L., 1999. Role of iron, light, and silicate in controlling algal biomass in subantarctic waters SE of New Zealand. J. Geophys. Res. 104, 13395–13408.

Boyd, P.W., et al., 2000. A mesoscale phytoplankton bloom in the polar Southern Ocean stimulated by iron fertilization. Nature 407, 695–702.

Boyd, P.W., Crossley, A.C., DiTullio, G.R., Griffiths, F.B., Hutchins, D.A., Queguiner, B., Sedwick, P.N., Trull, T.W., 2001. Control of phytoplankton growth by iron supply and irradiance in the subantarctic Southern Ocean: experimental results from the SAZ project. J. Geophys. Res. 106, 31573–31583.

Brown, S.L., Landry, M.R., 2001. Mesoscale variability in biological community structure and biomass in the Antarctic Polar Front region at 170°W during austral spring 1997. J. Geophys. Res. 106, 13917–13930.

Brown, J.W., Brown, O.B., Evans, R.H., 1993. Calibration of advanced very high resolution radiometer infrared channels: a new approach to nonlinear correction. J. Geophys. Res. 98, 18257–18268.

Chelton, D.B., Schlax, M.G., Witter, D.L., Richman, J.G., 1990. Geosat altimeter observations of the surface circulation of the Southern Ocean. J. Geophys. Res. 95, 17877–17903.

Coale, K.H., Johnson, K.S., Fitzwater, S.E., Gordon, R.M., Tanner, S., Chavez, F.P., Ferioli, L., Sakamoto, C., Rogers, P., Millero, F., Steinberg, P., Nightingale, P., Cooper, D., Cochlan, W.P., Landry, M.R., Constantinou, J., Rollwagen, G., Trasvina, A., Kudela, R., 1996. A massive phytoplankton bloom induced by an ecosystem-scale iron fertilization experiment in the equatorial Pacific Ocean. Nature 383, 495–501.

Comiso, J.C., McClain, C.R., Sullivan, C.W., Ryan, J.P., Leonard, C.L., 1993. Coastal Zone Color Scanner pigment concentrations in the Southern Ocean and relationships to geophysical surface features. J. Geophys. Res. 98, 2419–2451.

Dafner, E.V., Mordosova, N.V., 1994. Influence of biotic factors on the hydrochemical structure of surface water in the Polar Frontal Zone of the Atlantic Antarctic. Mar. Chem. 45, 137–148.

Daniault, N., Ménard, Y., 1985. Eddy kinetic energy distribution in the Southern Ocean from altimetry and FGGE drifting buoys. J. Geophys. Res. 90, 11877–11889.

Deacon, G.E.R., 1933. A general account of the hydrology of the South Atlantic Ocean. Discov. Rep. VII, 177–238.

de Baar, H.J.W., de Jong, J.T.M., Bakker, D.C.E., Löscher, B.M., Veth, C., Bathmann, U., Smetacek, V., 1995. Importance of iron for plankton blooms and carbon dioxide drawdown in the Southern Ocean. Nature 373, 412–415.

de Baar, H.J.W., Van Leeuwe, M.A., Scharek, R., Goeyens, L., Bakker, K.M.J., Fritsche, P., 1997. Nutrient anomalies in *Fragilariopsis kerguelensis* blooms, iron deficiency and the nitrate/phosphate ratio (A.C. Redfield) of the Antarctic Ocean. Deep-Sea Res. II 44, 229–260.

De La Rocha, C.L., Hutchins, D.A., Brzezinski, M.A., Zhang, Y., 2000. Effects of iron and zinc deficiency on elemental composition and silica production by diatoms. Mar. Ecol. Prog. Ser. 195, 71–79.

Flierl, G.R., Davis, C.S., 1993. Biological effects of Gulf Stream meandering. J. Mar. Res. 51, 529–560.

Frank, V.M., Brzezinski, M.A., Coale, K.H., Nelson, D.M., 2000. Iron and silicic acid concentrations regulate Si uptake north and south of the Polar Frontal Zone in the Pacific Sector of the Southern Ocean. Deep-Sea Res., Part II 47, 3315–3338.

Gall, M.P., Boyd, P.W., Hall, J., Safi, K.A., Chang, H., 2001. Phytoplankton processes: Part I. community structure during the Southern Ocean Iron Release Experiment (SOIREE). Deep-Sea Res., Part II 48, 2551–2570.

Gouretski, V.V., Danilov, A.I., 1993. Weddell Gyre: structure of the eastern boundary. Deep-Sea Res. 40, 561–582.

Gouretski, V.V., Danilov, A.I., 1994. Characteristics of warm rings in the African sector of the Antarctic Circumpolar Current. Deep-Sea Res. 41, 1131–1157.

Helbling, E.W., Villafañe, V., Holm-Hansen, O., 1991. Effect of

iron on productivity and size distribution of Antarctic phyto-plankton. Limnol. Oceanogr. 36, 1879–1885.

Hutchins, D.A., Bruland, K.W., 1998. Iron-limited growth and Si: N uptake ratios in a coastal upwelling regime. Nature 393, 561–564.

Hutchins, D.A., Sedwick, P.N., DiTullio, G.R., Boyd, P.W., Queguiner, B., Griffiths, F.B., Crossley, C., 2001. Control of phytoplankton growth by iron and silicic acid availability in the subantarctic Southern Ocean: experimental results from the SAZ project. J. Geophys. Res. 106, 31559–31572.

Hutchins, D.A., Hare, C.E., DiTullio, G.R., Crossley, A.C., Sedwick, P.N., 2002. Effects of iron limitation on Southern Ocean biogeochemistry and phytoplankton community structure assessed with a natural community continuous culture incubation system. EOS Trans. AGU 83 (4) (Ocean Sci. Meet. Suppl., Abstract S11L-02).

Jochem, F.J., Mathot, S., Quéguiner, B., 1995. Size-fractionated primary production in the open Southern Ocean in austral spring. Polar Biol. 15, 381–392.

Johnson, K.S., Chavez, F.P., Friederich, G.E., 1999. Continental-shelf sediment as a primary source of iron for coastal phytoplankton. Nature 398, 697–700.

Joyce, T.M., Zenk, W., Toole, J.M., 1978. The anatomy of the Antarctic Polar Front in the Drake Passage. J. Geophys. Res. 83, 6093–6113.

Kilpatrick, K.A., Podesta, G.P., Evans, R., 2001. Overview of the NOAA/NASA advanced very high resolution radiometer Pathfinder algorithm of sea surface temperature and associated matchup database. J. Geophys. Res. 106, 9179–9197.

Lancelot, C., Hannon, E., Becquevort, S., Veth, C., De Baar, H.J.W., 2000. Modeling phytoplankton blooms and carbon export production in the Southern Ocean: dominant controls by light and iron in the Atlantic sector in Austral spring 1992. Deep-Sea Res., Part I 47, 1621–1662.

Laubscher, R.K., Perisinotto, R., Mcquaid, C.D., 1993. Phytoplankton production and biomass at frontal zones in the Atlantic sector of the Southern Ocean. Polar Biol. 13, 471–481.

Legeckis, R., 1977. Oceanic Polar Front in the Drake Passage—satellite observations during 1976. Deep-Sea Res. 24, 701–704.

Löscher, B.M., de Baar, H.J.W., de Jong, J.T.M., Veth, C., Dehairs, F., 1997. The distribution of Fe in the Antarctic Circumpolar Current. Deep-Sea Res., Part II 44, 143–187.

Lutjeharms, J.R.E., Walters, N.M., Allanson, B.R., 1985. Oceanic frontal systems and biological enhancement. In: Siegfried, W.R., Condy, P.R., Laws, R.M. (Eds.), Antarctic Nutrient Cycles and Food Webs. Springer-Verlag, Berlin, pp. 11–21.

Mackintosh, N.A., 1946. The Antarctic Convergence and the distribution of surface temperatures in Antarctic waters. Discov. Rep. XXIII, 177–212.

Martin, J.H., 1990. Glacial-interglacial CO$_2$: the iron hypothesis. Paleoceanography 5, 1–13.

Martin, J.H., Fitzwater, S.E., Gordon, R.M., 1990a. Iron in Antarctic waters. Nature 345, 156–158.

Martin, J.H., Fitzwater, S.E., Gordon, R.M., 1990b. Iron deficiency limits phytoplankton growth in Antarctic waters. Glob. Biogeochem. Cycles 4, 5–12.

McClain, C.R., Cleave, M.L., Feldman, G.C., Gregg, W.W.,

Hooker, S.B., Kuring, N., 1998. Science quality SeaWiFS data for global biosphere research. Sea Technol., 10–16 (September).

Measures, C.I., Vink, S., 2001. Dissolved Fe in the upper waters of the Southern Ocean during the 1997/1998 US-JGOFS cruises. Deep-Sea Res., Part II 48, 3913–3941.

Mengelt, C., Abbott, M.R., Barth, J.A., Letelier, R.M., Measures, C.I., Vink, S., 2001. Phytoplankton pigment distributions in relation to silicic acid, iron and the physical structure across the Antarctic Polar Front, 170°W, during austral summer. Deep-Sea Res., Part II 48, 4081–4100.

Mitchell, B.G., Brody, E.A., Holm-Hansen, O., McClain, C., Bishop, J., 1991. Light limitation of phytoplankton biomass and macro-nutrient utilization in the Southern Ocean. Limnol. Oceanogr. 36, 1662–1677.

Moore, J.K., Abbott, M.R., Richman, J.G., 1997. Variability in the location of the Antarctic Polar Front (90°–20°W) from satellite sea surface temperature data. J. Geophys. Res. 102, 27825–27833.

Moore, J.K., Abbott, M.R., 2000. Phytoplankton chlorophyll distributions and primary production in the Southern Ocean. J. Geophys. Res. 105, 28709–28722.

Moore, J.K., Abbott, M.R., Richman, J.G., 1999a. Location and dynamics of the Antarctic Polar Front from satellite sea surface temperature data. J. Geophys. Res. 104, 3059–3073.

Moore, J.K., Abbott, M.R., Richman, J.G., Smith, W.O., Cowles, T.J., Coale, K.H., Gardner, W.D., Barber, R.T., 1999b. SeaWiFS satellite ocean color data from the Southern Ocean. Geophys. Res. Lett. 26, 1465–1468.

Moore, J.K., Abbott, M.R., Richman, J.G., Nelson, D., 2000. The Southern Ocean at the Last Glacial Maximum: a strong sink for atmospheric carbon dioxide. Glob. Biogeochem. Cycles 14, 455–475.

Moore, J.K., Doney, S.C., Glover, D.M., Fung, I.Y., 2002. Iron cycling and nutrient limitation patterns in surface waters of the world ocean. Deep-Sea Res., Part II 49, 463–508.

Morrow, R., Coleman, R., Bhurch, J., Chelton, D., 1994. Surface eddy momentum flux and velocity variances in the Southern Ocean from Geosat altimetry. J. Phys. Oceanogr. 24, 2050–2071.

Nelson, D.M., Smith Jr., W.O., 1991. Sverdrup revisited: critical depths, maximum chlorophyll levels, and the control of Southern Ocean productivity by the irradiance-mixing regime. Limnol. Oceanogr. 36, 1650–1661.

Nelson, D.M., Brzezinski, M.A., Sigmon, D.E., Frank, V.M., 2001. A seasonal progression of Si limitation in the Pacific sector of the Southern Ocean. Deep-Sea Res., Part II 48, 3973–3995.

Nolting, R.F., de Baar, H.J.W., Van Bennekom, A.J., Masson, A., 1991. Cadmium, copper and iron in the Scotia Sea, Weddell Sea, and Weddell/Scotia Confluence (Antarctica). Mar. Chem. 35, 219–243.

Olson, D.B., Hitchcock, G.L., Mariano, A.J., Ashjian, C.J., Peng, G., Nero, R.W., Podestá, G.P., 1994. Life on the edge: marine life and fronts. Oceanography 7, 52–60.

Orsi, A.H., Whitworth III, T., Nowlin Jr., W.D., 1995. On the meridional extent and fronts of the Antarctic Circumpolar Current. Deep-Sea Res., Part I 42, 641–673.

Peterson, R.G., Whitworth III, T., 1989. The Subantarctic and Polar Fronts in relation to deep water masses through the southwestern Atlantic. J. Geophys. Res. 94, 10817–10838.

Pollard, R.T., Regier, L.A., 1992. Vorticity and vertical circulation at an ocean front. J. Phys. Oceanogr. 22, 609–625.

Pollard, R.T., Read, J.F., Allen, J.T., Griffiths, G., Morrison, A.I., 1995. On the physical structure of a front in the Bellingshausen Sea. Deep-Sea Res., Part II 42, 955–982.

Price, N.M., Ahner, B.A., Morel, F.M.M., 1994. The equatorial Pacific Ocean: Grazer-controlled phytoplankton populations in an iron-limited system. Limnol. Oceanogr. 39, 520–534.

Read, J.F., Pollard, R.T., Morrison, A.I., Symon, C., 1995. On the southerly extent of the Antarctic Circumpolar Current in the southeast Pacific. Deep-Sea Res., Part II 42, 933–954.

Sandwell, D.T., Zhang, B., 1989. Global mesoscale variability from the Geosat exact repeat mission: correlation with ocean depth. J. Geophys. Res. 94, 17971–17984.

Sedwick, P.N., Edwards, P.R., Mackey, D.J., Griffiths, F.B., Parslow, J.S., 1997. Iron and manganese in surface waters of the Australian subantarctic region. Deep-Sea Res., Part I 44, 1239–1253.

Sedwick, P.N., DiTullio, G.R., Hutchins, D.A., Boyd, P.W., Griffiths, F.B., Crossley, A.C., Trull, T.W., Quéguiner, B., 1999. Limitation of algal growth by iron deficiency in the Australian Subantarctic region. Geophys. Res. Lett. 26, 2865–2868.

Sedwick, P.N., DiTullio, G.R., Mackey, D.J., 2000. Iron and manganese in the Ross Sea, Antarctica: seasonal iron limitation in Antarctic shelf waters. J. Geophys. Res. 105, 11321–11336.

Selph, K.E., Landry, M.R., Allen, C.B., Calbet, A., Christensen, S., Bidigare, R.R., 2001. Microbial community composition and growth dynamics in the Antarctic Polar Front and seasonal ice zone during late spring 1997. Deep-Sea Res., Part II 48, 4059–4080.

Sherr, E.B., Sherr, B.F., 1994. Bacterivory and herbivory: key roles of phagotropic protists in pelagic food webs. Microb. Ecol. 28, 223–235.

Smetacek, V., de Baar, H.J.W., Bathmann, U.V., Lochte, K., Rutgers van der Loeff, M.M., 1997. Ecology and biogeochemistry of the Antarctic Circumpolar Current during austral spring: a summary of Southern Ocean JGOFS cruise ANT X/6 of R.V. *Polarstern*. Deep-Sea Res., Part II 44, 1–21.

Smith Jr., W.O., Nelson, D.M., 1986. Importance of ice edge phytoplankton production in the Southern Ocean. BioScience 36, 251–257.

Smith, W.H.F., Sandwell, D.T., 1994. Bathymetric prediction from dense satellite altimetry and sparse shipboard bathymetry. J. Geophys. Res. 99, 21803–21824.

Smith, E., Vazquez, J., Tran, A., Sumagaysay, R., 1996. Satellite-derived sea surface temperature data available from the NOAA/NASA Pathfinder Program. Eos Trans. AGU Electron. Suppl. (April 2) (Available as http://www.agu.org/eos_elec/95274e.html).

Smith, W.O., Anderson, R.F., Moore, J.K., Codispoti, L.A., Morrison, J.M., 2000. The U.S. Southern Ocean Joint Global Ocean Flux Study: an introduction to AESOPS. Deep-Sea Res., Part II 47, 3073–3093.

Sullivan, C.W., Arrigo, K.R., McClain, C.R., Comiso, J.C., Firestone, J., 1993. Distributions of phytoplankton blooms in the Southern Ocean. Science 262, 1832–1837.

Sunda, W.G., Huntsman, S.A., 1997. Interrelated influence of iron, light, and cell size on marine phytoplankton growth. Nature 390, 389–392.

Takeda, S., 1998. Influence of iron availability on nutrient consumption ratio of diatoms in oceanic waters. Nature 393, 774–777.

Trathan, P.N., Brandon, M.A., Murphy, E.J., 1997. Characterization of the Antarctic Polar Frontal Zone to the north of South Georgia in summer 1994. J. Geophys. Res. 102, 10483–10497.

Trathan, P.N., Brandon, M.A., Murphy, E.J., Thorpe, S.E., 2000. Transport and structure within the Antarctic Circumpolar Current to the north of South Georgia. Geophys. Res. Lett. 37, 1727–1730.

Tréguer, P., Jacques, G., 1992. Dynamics of nutrients and phytoplankton, and fluxes of carbon, nitrogen, and silicon in the Antarctic Ocean. Polar Biol. 12, 149–162.

Van Leeuwe, M.A., Scharek, R., de Baar, H.J.W., de Jong, J.T.M., Goeyens, L., 1997. Iron enrichment experiments in the Southern Ocean: physiological responses of plankton communities. Deep-Sea Res., Part II 44, 189–208.

Veth, C., Peeken, I., Scharek, R., 1997. Physical anatomy of fronts and surface waters in the ACC near 6°W meridian during austral spring 1992. Deep-Sea Res., Part II 44, 23–49.

Zeldis, J., 2001. Mesozooplankton community composition, feeding, and export production during SOIREE. Deep-Sea Res., Part II 48, 2615–2634.